NURETH14-073

INVESTIGATIONS ON FLOW INDUCED VIBRATION OF SIMULATED CANDU FUEL BUNDLES IN A PIPE

X. Zhang, and S.D. Yu

Ryerson University, Toronto, Ontario, Canada x8zhang@ryerson.ca, syu@ryerson.ca

Abstract

In this paper, vibration of a two-bundle string consisting of simulated CANDU fuel bundles subjected to turbulent liquid flow is investigated through numerical simulations and experiments. Large eddy simulation is used to solve the three-dimensional turbulent flow surrounding the fuel bundles for determining fluid excitations. The CFD model includes pipe flow, flow through the inlet fuel bundle along with its two endplates, half of the second bundle and its upstream endplate. The fluid excitation obtained from the fluid model is subsequently fed into a fuel bundle vibration code written in FORTRAN. Fluid structure interaction terms for the fuel elements are approximated using the slender body theory. Simulation results are compared to measurements conducted on the simulated fuel bundles in a testing hydraulic loop.

Keywords: vibration, fuel bundle, large eddy simulation.

1. Introduction

Unexpected high level of fuel bundle fretting and pressure tube wear were discovered in the CANDU reactors at the Bruce and Darlington sites in routine inspections and the investigations related to endplate failures [1]-[4]. Most significant fretting marks were found at the inlet of the fuel channels near the bearing pads of the inlet fuel bundle. Although strong acoustic pressure pulsation in particular fuel channels [5] was attributed for the severe vibration of fuel bundles and the failure of endplates, modest to severe wear marks were also found in majority of fuel channels where acoustic pulsation was not strong. Furthermore, the fretting level in the acoustically-active channels was reduced by replacing the primary heat transport pumps, but the replacement did not obviously reduce the fretting level in other channels [1][3]. In those acoustically-inactive channels, the local coolant flow is believed to be the most possible source of excitation. However, studies revealed that the small-scale turbulence in a fully developed flow inside the subchannels of a fuel bundle was not able to excite the fuel elements to vibrate at a level that would cause any excessive fretting marks on the pressure tubes [6]. Fluid-elastic instability may occur for isolated flexible cylinders in a parallel flow and lead to high level of vibration [7][8], but the mean flow velocity in the fuel channels in normal operations was far lower than the critical velocity for this type of instability to occur. Many in-reactor and out-reactor measurements were done [9][10], but the vibration mechanism and the source of excitation still remained undetermined.

[•] CANDU (CANada Deuterium Uranium), a registered trade mark of Atomic Energy of Canada Ltd (AECL).

The coolant enters the fuel bundle string from the upstream endplate of the inlet bundle. The abrupt change in the cross section area of the flow channel together with the presence of the endplate introduces disturbance in the flow. Eddies and wakes are generated after the inlet endplate and lead to fluctuations in the pressure and velocity field. The disturbance tends to die down with the development of the flow inside the bundle. At the downstream end of the inlet bundle, the flow is disturbed again by the endplates on the interface between the inlet and the second bundle. This pattern repeats until the end of the string. The flow regions are characterized in Figure 1.

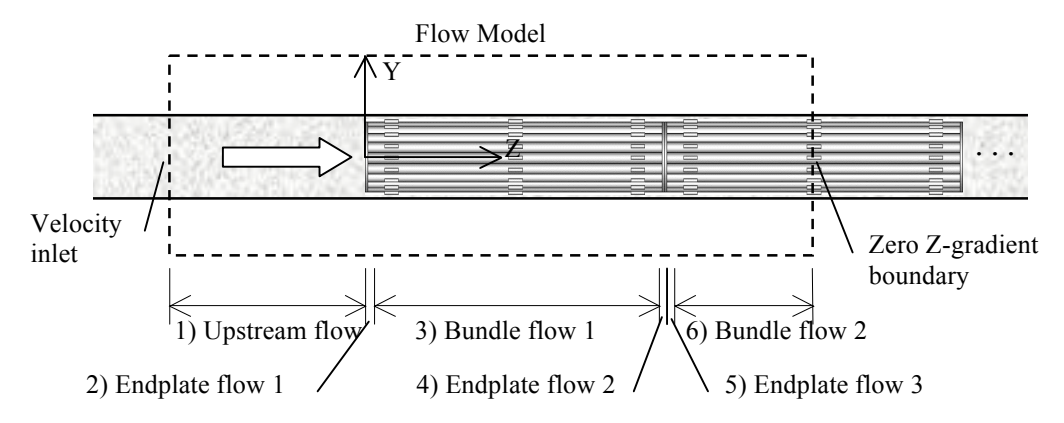


Figure 1 Schematic drawing of the inlet portion of a flow channel.

A challenge on the experimental study of the fuel channel flow is to measure the flow field without altering the flow. To date, only axial velocity measurement in a 37-element fuel bundle was done using a customized laser anemometry [11]. When fluid excitation is considered, it is necessary to obtain flow velocities in the transverse directions. Without knowing the fluctuation level of the fluid quantities of the disturbed flow, it is difficult to predict the response of the fuel bundles.

Computational fluid dynamics (CFD) can be used to overcome this difficulty. With the advance in large eddy simulation (LES) and computer technology, large scale numerical solution for the complex bundle flow can be obtained with controlled accuracy. LES uses grid-based spatial filters to separate large scale and small scale eddies [12]. Large scale eddies, which are responsible for the transport of most of the momentum and energy, are directly solved; and the small scale eddies are modelled. The large eddies are geometry-dependent and unsteady in nature. As a result, the direct solution of the large eddies provides better accuracy in modeling the fluid motion in complex flow situations. Modeling of small scale eddies, known as subgrid-scale (SGS) modeling [13], allows less computational effort than the direct solution of the Navier-Stokes equations. Theory of LES has been presented in a good number of articles and books, such as [14] and [15]. Applicability of LES on solving the flow passing through a 43-element CANDU fuel bundle was examined recently [16]. The method was found reliable and affordable.

A CANDU fuel bundle, shown in Figure 2, is designed to have a number of fuel elements radially and circumferentially spaced in a few concentric rings. The fuel elements are welded to an endplate at each end. The two endplates hold the fuel elements and make the fuel bundle an integral structure. Bearing pads are welded onto the outermost ring of fuel elements to maintain a healthy radial gap between a fuel bundle and the pressure tube over large areas of the fuel bundle exterior surfaces. As a structure, each fuel bundle can exhibit many vibration modes in a narrow span of frequencies. The fuel bundle need to be modelled as an integral structure, and this requires an accurate and efficient finite element model of the fuel bundles to de developed. One difficulty in developing such a model is the endplate. Conventional plate theory leads to large error due to the large thickness-to-width

ratio of the endplate ribs/webs and rings. The beam theory, however, cannot handle the material overlapping between the rings and the ribs/webs. The authors have developed an endplate model for the 43-element fuel bundle using a special thick plate element based on Reddy's third order plate theory ^[17]. The endplate model was found to be both accurate and efficient. It is then utilized together with a three-node Bernoulli beam element for fuel elements to build a dynamic model for the fuel bundles.

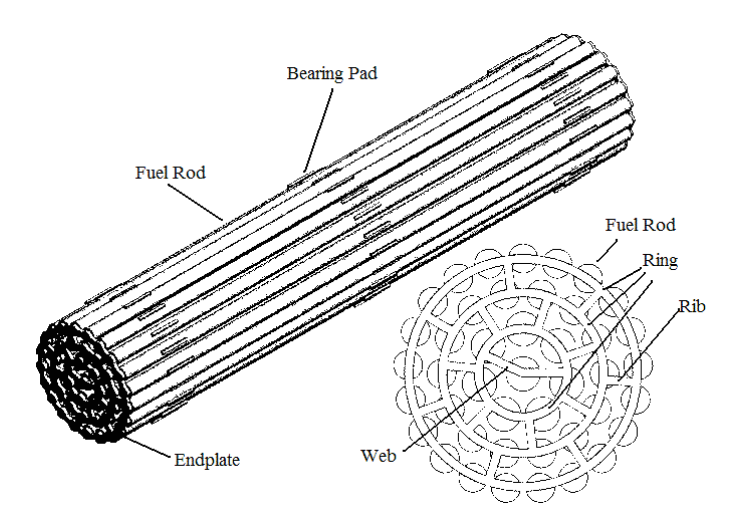


Figure 2 Illustration of a 43-element fuel bundle.

This paper presents some recent work on the fluid excitation and structure response in a short fuel string. The research is focused on the inlet fuel bundle since the most significant wear is found near the bearing pads of the inlet bundle. A hydraulic loop with two simulated fuel bundles was built to perform experiments. Computational models are developed to study the three-dimensional turbulent bundle flow and the structural response for the simulated bundles. An in-house finite element code is developed to model the fuel bundles. Fluid-structure interaction forces on the fuel elements in the parallel flow are incorporated in the fuel bundle model using the slender body theory [18]. The response of a fuel bundle at the inlet of a fuel string under the fluid excitation is obtained and compared with experiments.

2. Simulation of the Bundle Flow

The flow model is built and solved using FLUENT* 6. The global inertia frame is chosen as shown in Figure 1. The X-Y plane aligns with the upstream face of the upstream endplate of the inlet bundle with Z-axis coinciding with the longitudinal axis of the bundle. The interested flow condition, or the global Reynolds number inside the bundle, is about 54000. This Reynolds number corresponds to an average flow velocity of 3.0 m/s in the upstream pipe flow and an average flow velocity of 6.8 m/s inside the bundle. The global hydraulic diameter of the bundle flow is calculated to be $D_h \approx 0.008$ m. This presents the average hydraulic diameter of the subchannels. The density of the fluid (water) is $\rho = 1000 \text{ kg/m}^3$, and the kinematic viscosity is $v = 1 \times 10^{-6} \text{ m}^2/\text{s}$.

The three-dimensional CFD model consists of six regions: 1) the upstream pipe flow region; 2) the flow passing the upstream endplate of the first bundle; 3) the flow around the fuel elements of the first bundle; 4) the flow passing the downstream endplate of the first bundle; 5) the flow passing the

[•] FLUENT is a registered trademark of ANSYS Inc.

upstream endplate of the second bundle; 6) the flow inside the second bundle. These regions are shown in Figure 1. The upstream flow includes the pipe flow of $6D_p$, where D_p is the pipe diameter and its value is 0.1016 m (4 inch).

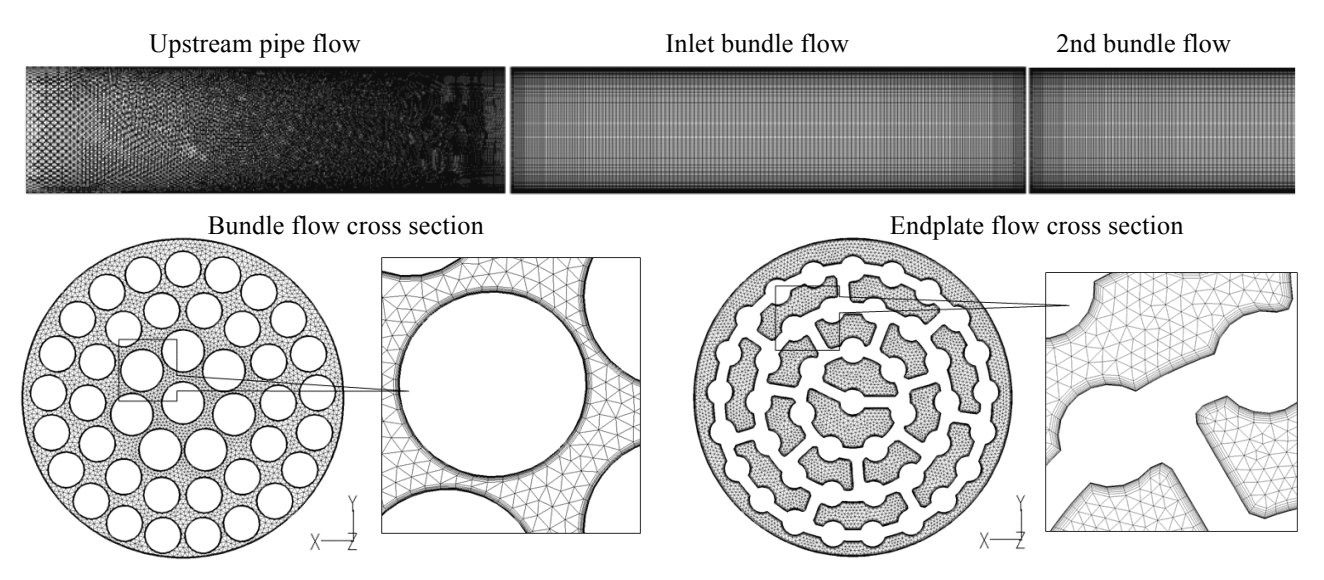


Figure 3 Mesh of the flow simulation model.

The regions are meshed individually, and non-conformable mapping is used to transfer data from one region to another. The mesh is shown in Figure 3. Wedge grid is used. The axial discretization interval is 3 mm in average in a bundle. Finer discretization is used near the endplates, in which the grid length is about 1.5 mm. The mesh near the midplanes of the bundles is coarser, with a length of 4.5 mm. The bundle flow cross section is discretized using a very fine mesh with the maximum mesh size lower than 1.5 mm in all directions. In the near wall region, 10 thin layers of hexahedron grids with a thickness growing factor of 1.3 are used near the fuel element surfaces and the pipe surface to simulate the boundary layer. The thickness of the first layer is 0.01 mm, which corresponds to y+=1 (dimensionless wall distance) on most surfaces, except in the vicinity of the leading edges of the fuel elements. The total number of cells in the model is 5.4 million. Compromise on grid quality is made to limit the size of the model so that it is affordable with the available computational resource, such as the coarse transition from the near wall grids to the core flow region. However, the near wall grids cover the buffer layer and some of the outer layer. No significantly high level of unreal dissipation is found at the transition region between the near wall grids and the core flow grids. However, this grid is not a typical grid that strictly fulfils LES requirements. The upstream boundary condition is set to velocity inlet, with a uniform velocity of 3 m/s. The downstream boundary condition is set to "outflow" boundary condition, in which the Zgradient of velocity and pressure at the boundary is zero.

The flow is solved in the time domain. The time step is determined based on the turbulent time scale $^{[19]}$ as $\tau \sim l\widetilde{u}^{-1}\,\mathrm{Re}^{-1/2} = 4\times10^{-5}\,\mathrm{s}$, where $l=D_h=0.008\,\mathrm{m}$, and \widetilde{u} is the fluctuating velocity whose value is estimated to be 10% of the mean flow velocity of $U=6.8\,\mathrm{m/s}$. This leads to a sampling frequency of 25000 Hz. According to the Nyquist sampling theorem, the highest frequency that a periodic signal can be reconstructed without aliasing problem is half of the sampling frequency, which is 12500 Hz in the current situation. However, the maximum discernable frequency related to the transportation of eddies depends on the eddy convective velocity U_c , the mesh size d_m , and the number of spatial points to represent a wave. The convective velocity, in the boundary layer of a pipe flow is approximately equal to 0.6 times of the mean flow velocity $^{[20]}$. If a wave can be

represented by 2 spatial points (or 2 mesh grids) according to the Nyquist sampling theorem, the highest frequency that can be discerned is determined by $f = U_c / (2d_m)$. For the average mesh size of 3 mm along the bundle axis, this frequency is about 680 Hz.

The flow model was solved using parallel processing on a high performance computing network. Each simulation involves 24 processors and 192 GB memory. A steady-state solution based on the k- ϵ with enhanced wall function is first sought. Then the LES is started from the steady-state solution and run for 1 second of flow time. The flow passing time for is about 0.16 second. The first 0.8 second of flow time (5 times of the flow passing time) is skipped because the flow is in the transition from the steady-state solution to a stable transient solution. Then the solution of 0.2 second starting from 0.8 second is processed. The contours of the velocity magnitude in the Y-Z plane at the entrance of the inlet bundle and the bundle interface are shown in Figure 4.

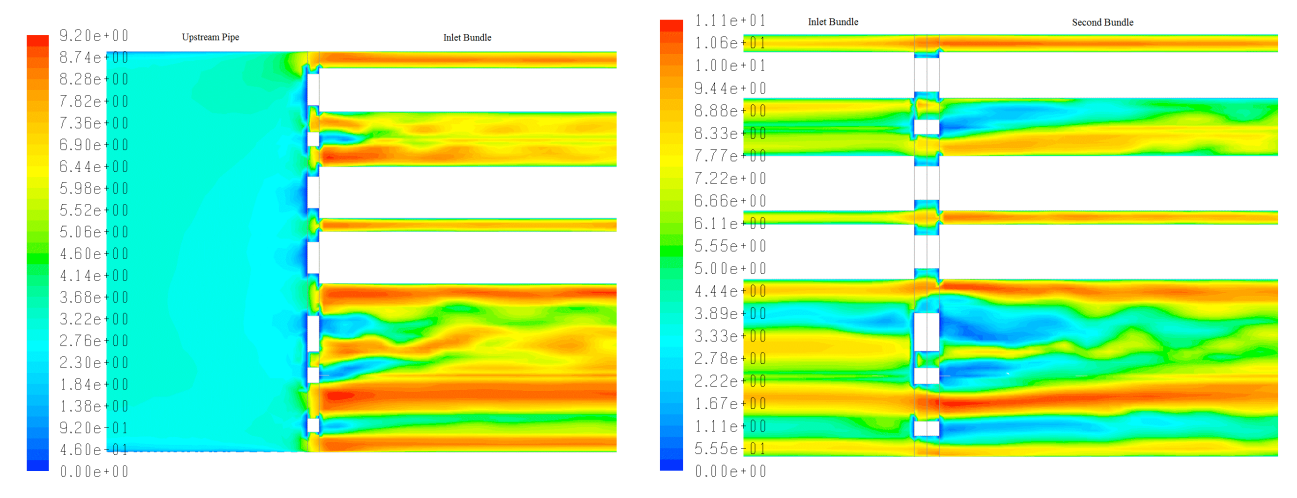


Figure 4 Velocity magnitude contour in the Y-Z plane at the entrance of the inlet bundle (left) and the bundle interface (right) at *t*=0.16 s.

It can be seen that the flow is disturbed by the endplates at both locations due to the presence of ribs and rings. Large wakes and vortices are generated after the rings and ribs (represented by small white rectangular boxes). The vortices are transported downstream to a significant distance. The vortices introduce fluctuations in the pressure field on the surfaces of the fuel elements and the endplates. The fluid force and moment acting on the fuel element and endplate are consequently fluctuating. Figure 5 shows the distribution of the root-mean-square (RMS) value of the overall fluid force in the X- and Y-direction and the moment in the Z-direction along the inlet bundle. It is clearly shown that the fluctuation of the force and the moment is significant near the endplates, while the fluctuation near the bundle midplane is far smaller. This indicates that the endplates is a significant source of excitation for fuel bundle vibration. The time histories and power spectral densities (PSDs) of the resultant X-force, Y-force, and Z-moment are shown in Figure 6. Spikes around 40 Hz and 200 Hz are seen in the X- and Y-force PSDs; for the Z-moment, most energy is distributed in a low frequency range below 50 Hz.

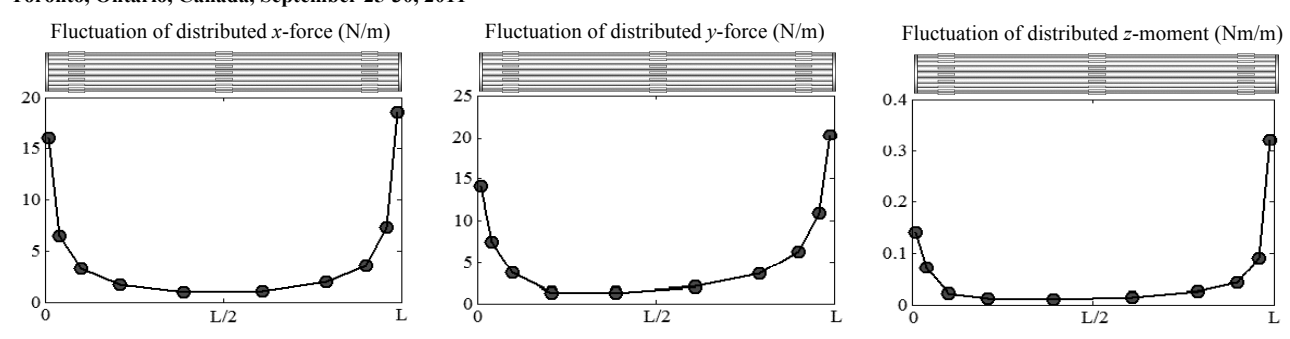


Figure 5 Root-mean-square fluctuation of the distributed fluid force on the inlet bundle.

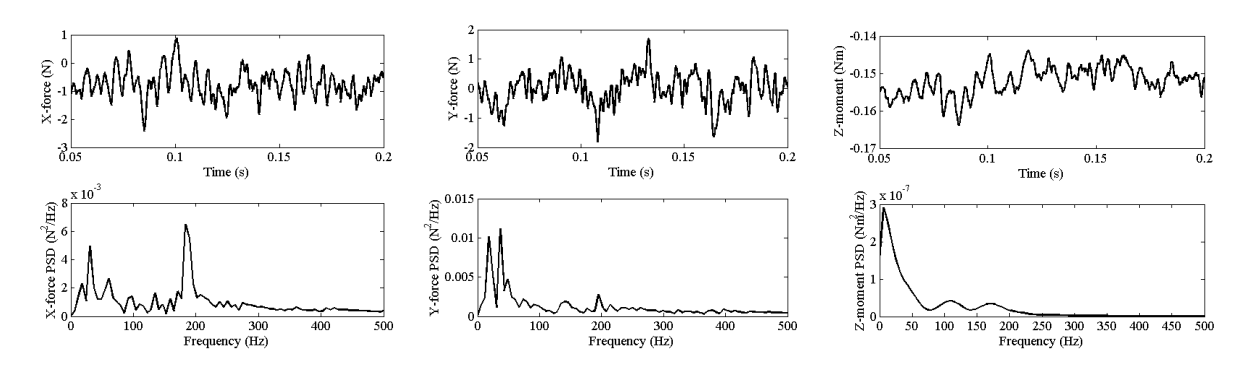


Figure 6 Time histories and PSDs of the resultant X-force, Y-force, and Z-moment on the inlet bundle.

3. Finite Element Model of Fuel Bundles

The fuel elements in the simulated bundles are solid beams with a length-to-diameter ratio of about 38. The Euler-Bernoulli beam theory ^[21] is used to model the fuel elements. A three-node three-dimensional Euler-Bernoulli beam element with bending-torsion coupling is developed. The endplates are meshed using a nine-node thick plate element developed by the authors ^[17]. The endplate mass is omitted, because its mass is negligible compared to that of the entire fuel bundle and the high frequency local modes of the endplate ribs/rings are not of interest in this application. The endplates are then substructured into endplate super-elements. Joint of the beam element and the endplates are implemented using constraint equations by taking force and moment balance on their interface. The endplate mesh, the super-element, and the bundle mesh are shown in Figure 7.

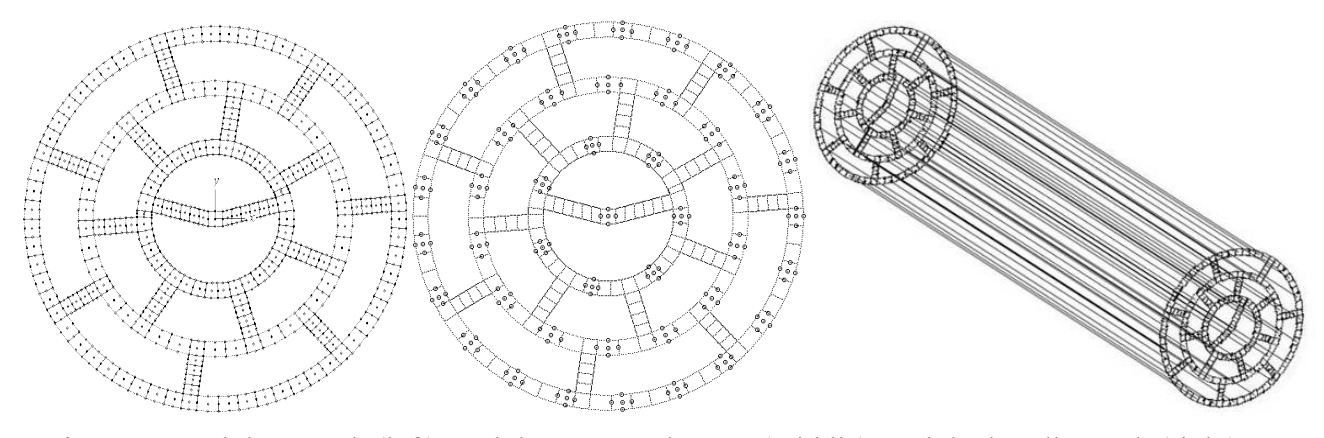


Figure 7 Endplate mesh (left), endplate super-element (middle), and the bundle mesh (right).

4. Simulation of Vibration of Inlet Bundle

Fluid-structure interaction needs to be considered when modelling the fuel bundle vibration in a fluid flow. In the current application, weak coupling is assumed based on the following reasons. Experiments show that the bundle vibration displacement is less than 0.1 mm under the highest flow rate. This amplitude is far smaller than the diameters of the fuel elements (11 and 13 mm) and the cross-sectional dimension of the subchannels (5~15 mm). The change on the geometry of the flow channels caused by the motion of the bundle is therefore negligible. The vibration velocity amplitude is also found in the order of 1 mm/s, which is far smaller than the average flow velocity of 6.8 m/s in the bundle, and even much smaller than the flow velocity oscillation caused by the large scale turbulence. Therefore, the influence of the structural motion to the solution of the fluid field is small. This allows the fluid field to be solved for fluid excitation without considering the bundle motion. However, the dynamic properties of the bundle are significantly influenced by the presence of the flow due to the added mass and the fluid damping. These terms come from the reaction force of a fluid field to the structure motion, and can be obtained by analytical solution of a simpler fluid field. Based on the slender body theory, the added terms for each fuel element can be expressed in the following forms [7] [18]. The added inertial terms in the X- and Y-direction are

$$f_x^{am} = \chi \rho A \frac{\partial^2 u}{\partial t^2}; \ f_y^{am} = \chi \rho A \frac{\partial^2 v}{\partial t^2}. \tag{1}$$

The added stiffness terms in the X- and Y-direction are

$$f_x^{as} = U^2 \frac{\partial^2 u}{\partial x^2} + 0.5\rho DUC_N U \frac{\partial u}{\partial x}; \quad f_y^{as} = U^2 \frac{\partial^2 v}{\partial x^2} + 0.5\rho DUC_N U \frac{\partial v}{\partial x}. \tag{2}$$

The fluid damping terms are

$$f_x^{ad} = 0.5\rho D(UC_N + C_D)\frac{\partial u}{\partial t} + U(1 + \chi \rho A)\frac{\partial^2 u}{\partial x \partial t}; f_y^{ad} = 0.5\rho D(UC_N + C_D)\frac{\partial v}{\partial t} + U(1 + \chi \rho A)\frac{\partial^2 v}{\partial x \partial t}.$$
(3)

In the above terms, U is the average flow velocity in the bundle. χ is the added mass coefficient due to confinement. Its value can be calculated as $\chi = (D_{ch}^2 + D_r^2)/(D_{ch}^2 - D_r^2)$; D_{ch} is the average subchannel diameter, estimated as 16 mm in the bundle; D_r is the average cylinder diameter, estimated to be 12 mm; ρ is the fluid density; A is the cross-sectional area of the cylinder; D is the diameter of the cylinder; C_N is the viscous drag coefficients in the lateral direction; C_D is the viscous drag coefficient in quiescent flow. The value of C_N is chosen as 0.02 based on the empirical data in the literature [23] [24]. The value of C_D is taken to be 0.1.

The system equations of motion can be expressed in a form of

$$\mathbf{M}_{sys}\ddot{\overline{\mathbf{u}}}(t) + \mathbf{C}_{sys}\dot{\overline{\mathbf{u}}}(t) + \mathbf{K}_{sys}\overline{\mathbf{u}}(t) = \mathbf{F}(t); \tag{4}$$

where $\overline{\mathbf{u}}$ represents the nodal displacement vector; $\mathbf{M}_{sys} = \mathbf{M}_s + \mathbf{M}_f$ and $\mathbf{K}_{sys} = \mathbf{K}_s + \mathbf{K}_f$ are the system mass and stiffness matrices, respectively; \mathbf{M}_s is the structural mass matrix; \mathbf{M}_f is the added mass matrix assembled from the beam elements; \mathbf{K}_s is the structural stiffness matrix; \mathbf{K}_f is the added stiffness matrix assembled from the beam elements; \mathbf{C}_i is the damping matrix representing

the damping effect introduced by the inviscid fluid force. C_v is the damping matrix representing the viscous damping. It is found that entries in K_f are negligible compared to those in K_s in the current application. $C_{svs} = C_i + C_v$ is the system damping matrix.

Equation (1) is converted into modal space using modal analysis. In a slightly damped system, a common approximation is to ignore the off-diagonal damping terms and keep the diagonal terms as the modal damping. With this approximation, the equations of motion can be decoupled into a set of single-degree-of-freedom equations:

$$\ddot{\eta}_{i}(t) + 2\zeta_{i}\omega_{i}\dot{\eta}_{i}(t) + \omega_{i}^{2}\eta_{i}(t) = m_{i}^{-1}Q_{i}(t); \quad (i=1,2,...,N_{m})$$
(5)

where m_i is the modal mass of the *i*-th mode; $\omega_i = \sqrt{k_i/m_i}$ is the natural frequency of the mode; $\zeta_i = c_i/(2m_i\omega_i)$ is the modal damping factor; η_i is the modal coordinate; $Q_i(t)$ is the modal excitation; N_m is the number of modes. Each of the above equations can be efficiently solved by the state transition matrix method [21].

A FORTRAN code has been developed to solve the above equations. The solution of 0.5 second in duration is sought with 100 modes retained in the solution. The displacement solution is obtained at the location where the sensor is mounted, and then the relative displacement between the sensor and the fuel element is calculated and plotted in Figure 8. The initial configuration of the sensor and the target fuel element is also shown in the figure. The fundamental mode is a low frequency mode in the range of 6 to 7 Hz. The motion of this mode is a rolling-like motion. This is mainly because the first bundle is separated from the second bundle with a roller and able to swing from side to side. Higher modes that are related to bending of fuel elements are also captured.

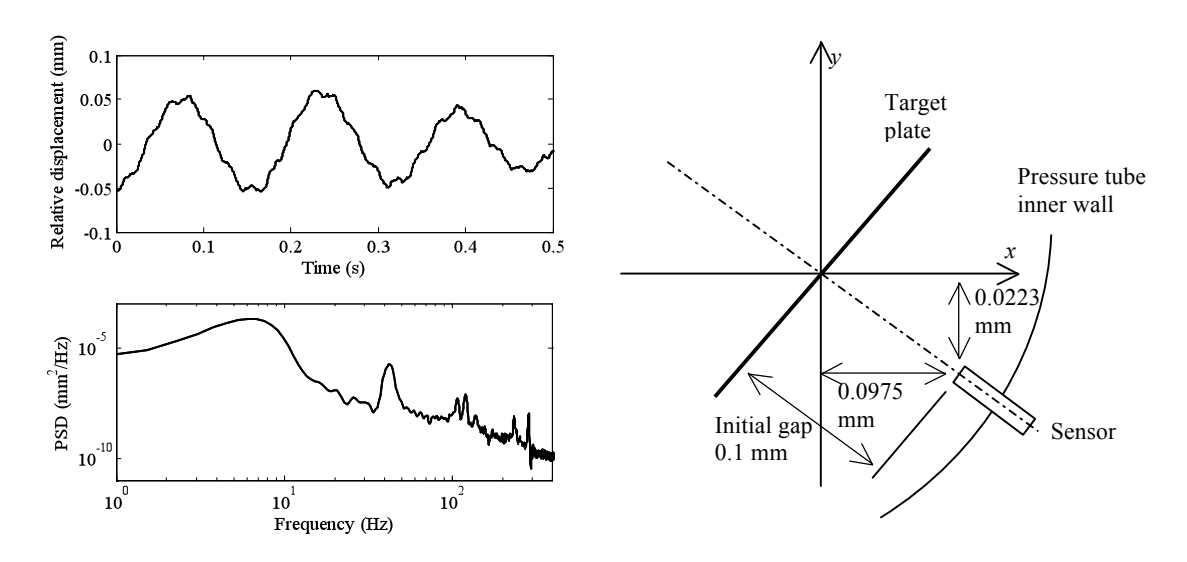


Figure 8 Time history and PSD of the relative displacement for 0.5 s record (left) and the sensor location (right).

5. Experiments

Experiments are done to validate the simulation results. A test rig, illustrated in Figure 9, consists of a 500 gallon tank, a 15 m PVC pipe loop, and a 10 horsepower centrifugal pump. The inner

diameter D_p of the pipe is 101.6 mm (4 inch). The test chamber, located before the vertical pipe that connected to the tank, is made of clear PVC pipe. The distance between the inlet of the test chamber and the elbow in the nearest upstream is $30D_p$. This allows the pipe flow to be fully developed before entering the test section. Two bundles are placed in the test section. These bundles are made with stainless steel. The geometry of the CFD model closely reflects that of the testing bundle except that four tiny bearing pads at the two bottom fuel elements on each bundle are not included. A shield plug is used to hold the bundle string against the flow. The second bundle is clamped to the shield plug. Fixture screws are used from the side at multiple locations to prevent it from moving. The purpose of using the second bundle is to eliminate wakes at the downstream of the inlet bundle. To avoid dealing frictional contact at the bundle-bundle interface, the inlet bundle is separated using a tiny roller from the second bundle. The roller prevents the inlet bundle from moving along the pipe but allows the motion in the lateral directions. The size of the roller is very small so the gap between the two bundles is not too large to significantly affect the flow. The pump provides a maximum mass flow rate of 25.7 kg/s when two bundles are present in the test chamber. Fresh water at room temperature is used as the fluid. Pressurization of 1.4 atmosphere pressure (142) kPa) is applied to eliminate air bubbles and cavitation. A magnetic flow meter is installed to record the mass flow rate.

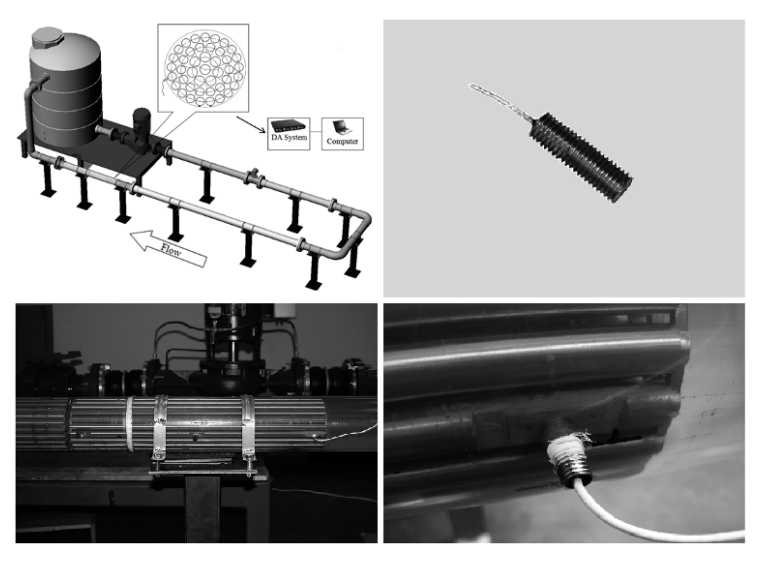


Figure 9 Experimental setup and the sensor location.

A non-contact displacement transducer (MicroStrain NC-DVRT-1.5) is installed at the location shown in Figure 9. The typical repeatability of this transducer is ±2 µm and the frequency range is 0 to 800 Hz. The voltage signals output from the sensor are collected by the HS4 multi-channel data acquisition system at a sampling rate of 1 kHz. The transducer only works with ferrous material and does not react to fuel elements made of stainless steel; therefore a small piece of steel plate is mounted on the monitored fuel element. The size of the steel plate is recommended by the manufacturer of the transducer and does not influence accuracy. The transducer was calibrated by the manufacturer with water as the working medium. The readout of the transducer is the relative displacement between the sensor and the target fuel element. The vibration of the bundle was recorded for 40 mass flow rates from 8.3 to 25.6 kg/s. The corresponding range of the average flow velocity in the bundle is 2.3 to 7.2 m/s. The record length for each measurement is 60 seconds.

The measured relative displacements between the transducer head and the target fuel element, together with their PSD, for three flow rates are shown in Figure 10. Note that the mean value of the

displacement has been deducted. The PSD is evaluated using Welch's method ^[22] with an overlapping of 50% and a Gaussian window applied to each data segment. The maximum displacement is about 0.1 mm for the highest flow velocity case, and 0.02 mm for the lowest flow rate case. The sharp spikes appearing at 60, 120, 180, 300 and 360 Hz are electric noise.

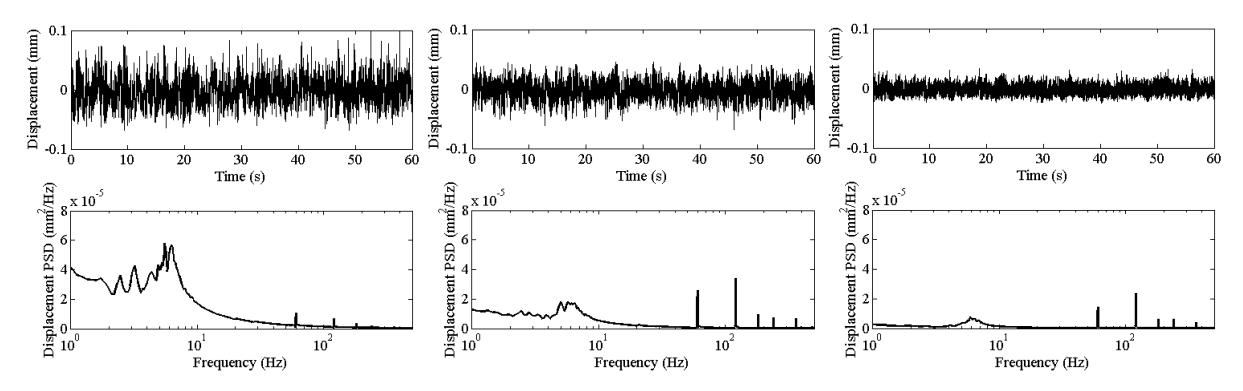


Figure 10 Measurement of the relative displacement under three flow rates: 25.6 kg/s (left), 17.8 kg/s (middle), and 11.4 kg/s (right).

A comparison between the measurement and the simulation for a flow rate of 24.2 kg/s (U=6.8 m/s) is shown in Figure 11. A reasonably good match can be seen between the simulation and the experimental result.

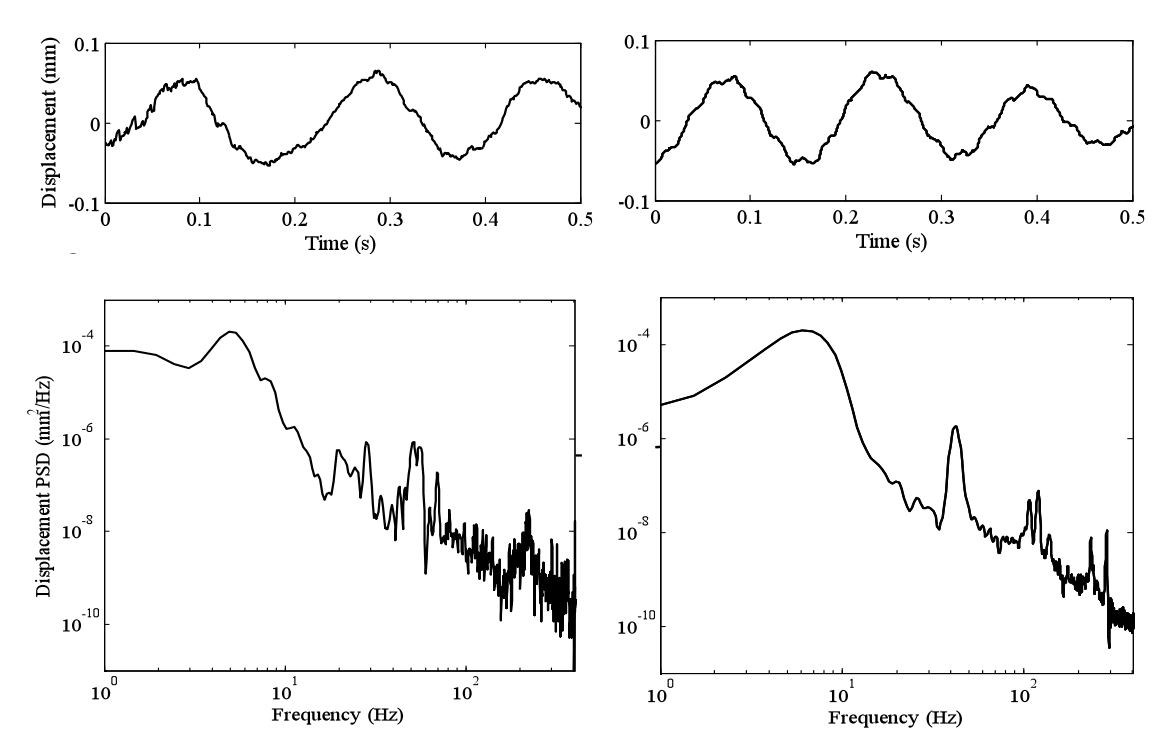


Figure 11 Comparison between experiment (left) and simulation (right).

6. Conclusion

This article presents the simulations and experiments of the vibrational response of the inlet fuel bundle in a two-bundle string in a simulated coolant loop. The three-dimensional turbulent flow

surrounding the fuel bundles is solved using the large eddy simulation. Numerical results show that large vortices are generated due to the presence of endplates. This pressure fluctuation is much more significant than that in the fully developed parallel bundle flow. This indicates that endplate may be the most important source of fluid excitation.

7. References

- [1] J. Judah, "Overview of fuel inspections at the Darlington nuclear generating station". <u>Proceedings of the 3rd International Conference on CANDU Fuel</u>, Chalk River, Ontario, Canada, 1992.
- [2] A.G. Norsworthy, G.J. Field, A. Meysner, K. Dalton, A. Crandell, "Fuel bundle to pressure tube fretting in Bruce and Darlington reactors". <u>Proceedings of the 15th CNS Annual Conference</u>, Montreal, Quebec, Canada, 1994.
- [3] A.G. Norsworthy, A. Ditschun, "Fuel bundle to pressure tube fretting in Bruce and Darlington", <u>Proceedings of the 16th CNS Annual Conference</u>, Saskatoon, Saskatchewan, Canada, 1995.
- [4] D. Dennier, A.M. Manzer, E. Kohn, "Characteristics of CANDU fuel bundles that caused pressure tube fretting at the bundle midplane". <u>Proceedings of the 16th CNS Annual Conference</u>, Saskatoon, Saskatchewan, Canada, 1995.
- [5] A. Misra, R.E. Pauls, D.K. Vijay, W. Teper, T.C. Lin, A. Strzelczyk, J. Liu, J., R. Hemraj, "Acoustic modeling in support of fuel failure investigation in a CANDU nuclear generating station", *American Society of Mechanical Engineers, Pressure Vessels and Piping Division, PVP*, Vol. 279, 1994, pp. 99-118.
- [6] M. Yetisir, N.J. Fisher, "Prediction of pressure tube fretting-wear damage due to fuel vibration", *Nuclear Engineering and Design*, Vol. 176, No. 3, 1997, pp. 261-271.
- [7] M.P. Paidoussis, "Dynamics of cylindrical structures subjected to axial flow", *Journal of Sound and Vibration*, Vol. 29, No. 3, 1973, pp. 365-385.
- [8] M.P. Paidoussis, J.P. Chaubernard, M.R. Genadry, K.N. El Barbir, "Dynamics of a cluster of flexible interconnected cylinders. Part 2. In axial flow", *Journal of Applied Mechanics*, Vol. 50, No. 2, 1983, pp. 429-435.
- [9] M.J. Pettigrew, "The vibration behavior of nuclear fuel under reactor conditions", *Nuclear Science and Engineering*, Vol. 114, No. 3, 1993, pp. 179-189.
- [10] B.A.W. Smith, D.D. Derken, "Measurement of steady and unsteady hydro-dynamic loads on a nuclear fuel bundle", *Journal of Fluids and Structures*, Vol. 12, No. 4, 1998, pp. 475-489.
- [11] D.F. D'Arcy, J.R. Schenk, "Axial velocity and turbulence measurements in adjacent subchannels of a 37-rod bundle", <u>Proceedings of 3rd International Symposium on Laser Anemometry</u>, Boston, US, 1987, pp. 277-282.
- [12] M. Germano, U. Piomelli, P. Moin, W.H. Cabot, "A dynamic subgrid-scale eddy viscosity model", *Physics of Fluids A*, Vol. 3, No. 7, 1991, pp. 1760-1765.
- [13] D.K. Lilly, "A Proposed Modification of the Germano Subgrid-Scale Closure Model", *Physics of Fluids A*, Vol. 4, No. 3, 1992, pp. 633-635.

- [14] H.K. Versteeg, W. Malalasekera, "An Introduction to Computational Fluid Dynamics the Finite Volume Method", <u>Pearson Education Limited</u>, Essex, England, 1995.
- [15] P. Sagaut, "Large Eddy Simulation for Incompressible Flow", <u>Springer-Verlag</u>, Berlin, Germany, 2006.
- [16] F. Abbasian, S.D. Yu, J. Cao, "Experimental and numerical investigations of three-dimensional turbulent flow of water surrounding a CANDU simulation fuel bundle structure inside a channel", *Nuclear Engineering and Design*, Vol. 239, No. 11, 2009, pp. 2224-2235.
- [17] X. Zhang, S.D. Yu, "A thick plate model for bending and twisting of CANDU fuel endplates", *Nuclear Engineering and Design*, Vol. 240, 2010, pp. 1565-1570.
- [18] R.D. Blevins, "Flow-Induced Vibration, 2nd Edition", <u>Krieger Publishing Company</u>, FL, USA, 1993.
- [19] H. Tennekes, J.L. Lumley, "A First Course in Turbulence", MIT Press, MA, USA, 1972.
- [20] J.M. Clinch, "Measurements of the wall pressure field at the surface of a smooth-walled pipe containing turbulent water flow", *Journal of Sound and Vibration*, Vol. 9, No. 3, 1969, pp. 398-419.
- [21] L. Meirovitch, "Fundamentals of Vibrations", McGraw Hill, NY, USA, 2001.
- [22] A.V. Oppenheim, R.W. Schafer, "Digital Signal Processing", Englewood Cliffs, NJ, USA, 1975.
- [23] S.F. Hoerner, "Fluid Dynamic Drag, 2nd edition", Hoerner Fluid Dynamics, Brick Town, NJ, USA, 1965.
- [24] C.R. Ortloff, J. Ives, "On the dynamic motion of a thin flexible cylinder in a viscous stream", *Journal of Fluid Mechanics*, Vol. 38, No. 4, 1969, pp. 713-720.